

## Plans for Spin Physics at RHIC

L.C. Bland

*Indiana University Cyclotron Facility, 2401 Sampson Road, Bloomington,  
IN 47408, USA*  
E-mail: [bland@iucf.indiana.edu](mailto:bland@iucf.indiana.edu)

Polarized proton collisions will be studied at RHIC up to a total center of mass energy of 500 GeV, starting in 2002. An overview of the RHIC-spin program, and the critical components of the PHENIX and STAR detectors for spin experiments, is presented. The premier experiment within the RHIC-spin program is the determination of the fraction of the proton's spin carried by gluons. A detailed analysis of how accurately this fraction can be determined by the STAR experiment at RHIC is presented.

### 1 Introduction

The purpose of this workshop is to establish the primary physics goals of a polarized electron-polarized ion collider (EPIC) that would become operational, at the earliest, in 2005. To predict what the most interesting questions will be *in the future*, it is necessary to understand what questions are being addressed in the present, and to establish the expected quality of the answers. With that perspective, I will describe plans for an experimental program at Brookhaven National Laboratory that will study the high-energy collisions of polarized protons, accelerated in the Relativistic Heavy Ion Collider (RHIC). There is great expectation within the community that the RHIC-spin program will provide us with important information about the spin structure of the proton. Arguably, the primary goal of the RHIC-spin experiments is to determine the fraction of the proton's spin carried by gluons (the integral  $\Delta G$ , defined below). Establishing the degree of polarization of the glue within the proton is the *next essential step* in understanding the spin structure of the proton. Under the assumption that experiments establishing the gluon polarization are the most important, most of this talk will be devoted to that subject.

### 2 An overview of the RHIC spin program

Before delving into the details about measuring the polarization of the proton's glue, it is important to give a broader overview of the physics of RHIC spin. To date, the highest energy achieved in a synchrotron for a polarized proton beam is 24.6 GeV in the AGS<sup>1</sup>. The RHIC rings will provide polarized proton

beams up to a maximum energy of  $\sim 250$  GeV, an order of magnitude higher in energy. Even more impressive is that the RHIC-spin program will provide total center of mass energy ( $\sqrt{s}$ ) for collisions between polarized protons up to 500 GeV. Furthermore, the expected luminosity for  $\vec{p} + \vec{p}$  collisions at RHIC ( $2 \times 10^{32} \text{ cm}^{-32} \text{ s}^{-1}$  at  $\sqrt{s} = 500$  GeV), will enable a systematic study of large transverse momentum ( $p_T$ ) processes, where perturbative QCD has been successfully applied to explain much of the data obtained at *unpolarized*  $pp$  and  $p\bar{p}$  colliders. The addition of polarization to high- $p_T$  collisions between protons at very high energies will provide an important test of QCD.

With the addition of polarization to colliding proton beams, *spin asymmetries* ( $A$ ):

$$PA = \frac{N_+ - N_-}{N_+ + N_-}, \quad (1)$$

are new observables that can be measured. In Eqn. 1, the beam polarization(s) are represented by  $P$  and are expected to be 70% for the RHIC-spin program. Asymmetry measurements are made by determining how the yield for some process varies with the polarization state ( $N_{\pm}$ ) of the beam(s) and by measuring the polarization of the beam(s). Eqn. 1 assumes equal integrated luminosities for the two polarization states of the beam(s). For the RHIC-spin program, it is expected that transverse single-spin asymmetries ( $A_T$ ) will approach zero for sufficiently large  $p_T$ ; non-zero values for  $A_T$  are expected only from higher-twist contributions. Parity-violating longitudinal single-spin asymmetries ( $A_L$ ) are expected to be quite large in the production of *real* weak bosons ( $W^{\pm}, Z^0$ )<sup>2</sup> or at sufficiently high  $p_T$ , where *virtual* weak bosons contribute significantly<sup>3</sup> to the force between the interacting partons.

Double-spin asymmetries involve differences of yields for a process when the initial state protons have the same and opposite direction polarizations. The (parity-allowed) longitudinal asymmetries ( $A_{LL}$ ) are expected to teach us about helicity asymmetry structure functions, similar to those probed in polarized deep inelastic scattering. Transverse double-spin asymmetries ( $A_{TT}$ ) may enable measurement of the transversity distributions<sup>5</sup>, related to the transverse polarization of the nucleon's constituents.

If QCD survives the onslaught of these new high-energy and high- $p_T$  polarization observables, then polarized proton collisions can be used as a tool to better understand the spin structure of the proton. As described in detail below,  $A_{LL}$  is very sensitive to the gluon polarization for several different processes. In addition, parity-violating  $A_L$  measurements for the production of  $W^{\pm}$  and  $Z^0$  can be directly related to the polarization of valence and sea quarks within the proton<sup>2</sup>. Since the valence quark polarizations are well determined in polarized deep inelastic scattering, direct tests of the Standard

Model are possible. By changing the kinematical conditions,  $\vec{p} + p \rightarrow W^\pm + X$  can be used to selectively probe antiquark polarizations, thereby providing new information about the proton's spin structure. Polarization observables for the highest  $p_T$  processes at RHIC may also provide limits on either the existence of new vector bosons or possible quark substructures<sup>3</sup>, competitive with planned measurements at the Tevatron.

### 3 Preparing RHIC for polarized proton studies

The RHIC spin program will present the opportunity to study observables in polarized  $pp$  collisions at  $\sqrt{s}$  values that are more than a factor of 25 larger than previously available<sup>4</sup>. This frontier of high-energy spin physics is made technically feasible by significant advances in the handling of polarized beams in synchrotrons and storage rings. The new technique employs so-called 'Siberian snakes', a concept introduced in Novosibirsk<sup>6</sup> and first experimentally verified at the IUCF Cooler ring<sup>7</sup>. The Siberian snake is a means of overcoming the large number of depolarizing resonances encountered when attempting to accelerate polarized proton (or other light ion) beams to high energies in a circular accelerator. For RHIC, helical dipole magnets, funded by the RIKEN institute in Japan, will be used to reverse the direction of unwanted transverse polarization components during alternate turns around each ring. In the absence of such spin manipulations, it is possible to destroy the beam polarization by small perturbations that act in a single turn, with their effects adding coherently when the ring is operated near a depolarizing resonance.

The motivation to build RHIC and its two major detectors, PHENIX and STAR, originated from the goal of discovering and studying a new state of matter, the *quark-gluon plasma*, that is thought to have existed at the earliest moments after the Big Bang. It is expected that the quark-gluon plasma should

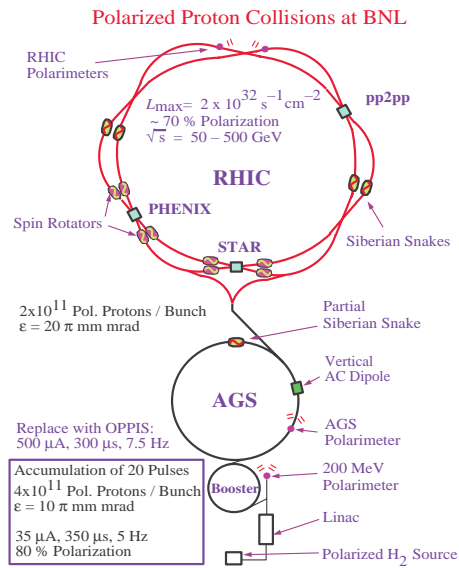


Figure 1: Schematic layout of the RHIC accelerator complex, indicating the critical elements needed for the acceleration of polarized ions.

be formed in the ultrarelativistic collisions between heavy-ion beams at RHIC. Although the major detectors were not designed for the study of  $\vec{p} + \vec{p}$  collisions up to total center of mass energy equal to 500 GeV, many of their subsystems have been subsequently adapted to this task. As a result, PHENIX and STAR bring complementary strengths to the RHIC-spin program.

The PHENIX detector has many relatively small acceptance detectors that provide fine granularity and precise particle identification. Of greatest relevance to the spin program are the photon arms that are centered at midrapidity ( $|\eta| \leq 0.35$ ), and the muon arms, spanning  $1.0 \leq |\eta| \leq 2.4$ . The fine granularity of the Pb-glass and Pb+scintillating fiber elements of the PHENIX electromagnetic calorimeter will provide the capability to separately identify single photons and di-photon pairs, produced in the decay of neutral mesons. These detectors will be employed for inclusive photon production in the RHIC-spin program. As well, they will be used to study high- $p_T \pi^0$  production. The muon arms provide excellent particle identification, and will be used for the study of  $W^\pm$  production, by observing the  $\mu^\pm$  daughters of the  $W$ . In addition, the detection of  $\mu^+ \mu^-$  pairs with the PHENIX muon arms will enable a program of measuring polarization observables associated with vector meson production and the Drell-Yan process.

The STAR detector is intended to provide a more global view of a heavy-ion collision. The heart of STAR is a 0.5 T solenoidal magnetic field and a time projection chamber (TPC), capable of tracking all of the charged particles produced in a central Au-Au collision in the nominal pseudorapidity interval,  $|\eta| \leq 2$ , with full azimuthal coverage. Multiple layers of silicon detectors around the interaction point will be used for reconstructing primary event vertices, and secondary vertices from strange particles. Of greatest relevance for the RHIC-spin program are the barrel and endcap electromagnetic calorimeters (EMC). Construction of the barrel EMC is underway and should be completed by 2002. A proposal<sup>8</sup> for the endcap EMC is awaiting final decision concerning funding. If approved, the construction timetable for that detector will be comparable to the barrel EMC project. In comparison to PHENIX, the STAR EMC has substantially coarser granularity, but provides full azimuthal coverage for the pseudorapidity interval,  $-1 \leq \eta \leq 2$ , with a small gap near  $\eta = +1$  for TPC and EMC services. The large acceptance of STAR makes it ideal for jet reconstruction. As described below, detection of photon + jet coincidences provides STAR with unique capabilities in determining  $\Delta G$ . In addition, measurements of di-jet production at STAR will provide an important cross check of the gluon polarization measured in direct photon production. Finally, the STAR EMC will also enable the study of  $W^\pm$  production, by observing the  $e^\pm$  daughters of the  $W$ .

As of July 1999, the status of the RHIC accelerator is as follows. Commissioning of Au beam in the RHIC rings began this summer. The initial studies of Au-Au collisions will commence in November 1999. The first helical dipole magnets have been successfully produced, and the initial commissioning of a polarized proton beam is scheduled for 2000. Initial studies of  $\vec{p} + \vec{p}$  collisions at low luminosity are planned for 2001. It is expected that full luminosity  $\vec{p} + \vec{p}$  collisions will begin in 2002. An agreement between RIKEN and BNL will allow the RHIC-spin program to run for 10 out of the 37 weeks of annual RHIC operations. It is projected that at full luminosity, a 10-week run at  $\sqrt{s}=200(500)$  GeV will result in an integrated luminosity of  $320(800)$  pb $^{-1}$ .

#### 4 Methods of determining $\Delta G$

After this brief overview of the spin-physics program and the tools to carry it out, I'll focus the rest of this writeup on the determination of the fraction of the proton's spin carried by gluons, which is expected to be the most important result forthcoming from the RHIC-spin program. That fraction is equal to twice the integral of the gluon helicity asymmetry distribution ( $\Delta G(x, Q^2)$ ):

$$\Delta G(Q^2) = \int_0^1 \Delta G(x, Q^2) dx = \int_0^1 [G^+(x, Q^2) - G^-(x, Q^2)] dx, \quad (2)$$

and is a function of the scale,  $Q^2$ . For convenience, I will subsequently suppress the dependence on  $Q^2$ . The asymmetry is given by the difference in probability of finding a gluon with its polarization parallel ( $G^+$ ) versus antiparallel ( $G^-$ ) to the proton's longitudinal polarization. The unpolarized gluon distribution function is given by  $G(x) = G^+(x) + G^-(x)$ . The gluon polarization is given by the ratio,  $\Delta G(x)/G(x)$ . Similar definitions of unpolarized parton distribution functions and helicity asymmetry distributions exist for quarks ( $q$ ) and antiquarks ( $\bar{q}$ ).

The importance of  $\Delta G$  is twofold. First, the proton's spin can be decomposed as follows:

$$S_z = \frac{1}{2} = \frac{1}{2} \Delta \Sigma + \Delta G + L_z^q + L_z^G. \quad (3)$$

Here,  $L_z^{q(G)}$  gives the orbital angular momentum contributions of quarks (gluons) to the proton's spin. The contribution quarks make to the proton's spin ( $\Delta \Sigma$ ) is determined from quark helicity asymmetry functions,  $\Delta q_i(x)$ , summed over the quark flavors ( $n_f$ ) consistent with  $Q^2$ , by:

$$\Delta \Sigma = \sum_{i=1}^{n_f} \Delta q_i, \text{ where } \Delta q_i = \int_0^1 [q_i^+(x) + \bar{q}_i^+(x) - q_i^-(x) - \bar{q}_i^-(x)] dx. \quad (4)$$

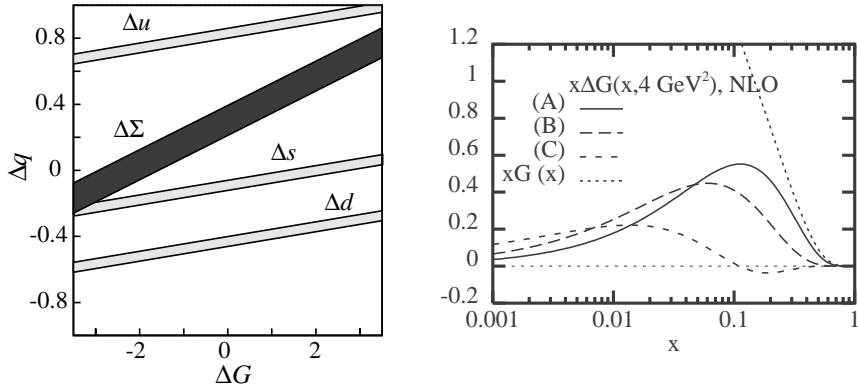


Figure 2: (Left) Correlation between the quark and gluon contributions to the proton's longitudinal polarization. (Right) Three models<sup>10</sup> of the gluon helicity asymmetry distribution.

Hence, if  $\Delta \Sigma$  is known, then a determination of  $\Delta G$  establishes the contribution of partonic orbital motion to the proton's spin.

The second reason for the importance of  $\Delta G$  is that, due to the axial anomaly of QCD, the quantity  $\Delta \Sigma$  *cannot be determined independently* of  $\Delta G$  in polarized deep inelastic scattering (PDIS). This is graphically illustrated in Fig. 2, showing the results from the global analysis of polarized deep-inelastic scattering (PDIS) made by the SMC group<sup>9</sup>. The analysis of the limited information on scaling violations in PDIS<sup>10</sup> has produced only crude constraints on  $\Delta G(x)$  and its integral.

The question then is, how can  $\Delta G$  be determined? There are several possible methods being pursued:

- Measurements of PDIS spanning a broad range of  $x$  and  $Q^2$  could be performed. A determination of  $\Delta G(x)$  would result from analysis of the scaling violations from this more extensive data set. This method would require a high-energy polarized  $ep$  collider. Possible plans for pursuing such a program at HERA were discussed at this workshop<sup>11</sup>.
- Measurement of the lepton production of di-jet events is sensitive to  $\Delta G(x)$  through the photon-gluon fusion process. A variation of this method is to detect high- $p_T$  charged hadron pairs, assumed to be the leading particles of jets, in high-energy polarized-lepton/polarized-proton collisions. This method is being pursued by COMPASS<sup>12</sup>, and intriguing data has already been obtained at much lower energy by HERMES<sup>13</sup>.

- Measurements of di-jet production, high- $p_T$  particle or photon production in  $\vec{p} + \vec{p}$  collisions are sensitive to  $\Delta G(x)$ . This is the primary focus of the RHIC-spin program.

Sensitivity to  $\Delta G(x)$  in polarized proton collisions arises for partonic collisions involving gluons. Di-jet production can be initiated either by  $qq$ ,  $qg$  or  $gg$  collisions, with the latter two possibilities involving  $\Delta G(x)$  linearly or quadratically, respectively. Just as for lepton-induced processes, detection of high- $p_T$  hadrons, assumed to be the particles of final-state jets, is also sensitive to  $\Delta G(x)$ . But, the relationship between the initial-state partonic kinematics and the hadron's  $p_T$  is more complex because of the momentum sharing between the multiple hadrons within the jets.

Direct photon production is, in principle, the cleanest probe of  $\Delta G(x)$  for  $\vec{p} + \vec{p}$  collisions, since in leading-order pQCD, observables are only linearly dependent on the gluon structure function for the dominant gluon Compton scattering process  $gq \rightarrow \gamma q$ . For  $pp \rightarrow \gamma X$ , there is only a small physics background from  $q\bar{q} \rightarrow \gamma g$ . Furthermore, when the photon is detected in coincidence with the away-side jet, the initial-state partonic kinematics can be reconstructed (see Sect. 5.3). Hence, direct photon production is a primary focus of the RHIC spin program.

## 5 Plans for determining $\Delta G$ at STAR

One of the most promising methods for determining  $\Delta G$  is to study direct photon production in polarized proton collisions. Both PHENIX and STAR will study this process for the RHIC-spin program. Below, I give a detailed assessment, somewhat biased towards the performance of the STAR detector, of how accurately  $\Delta G$  will be determined in polarized proton collisions at RHIC.

### 5.1 General features of direct photon production in $pp$ collisions

Within the framework of leading-order perturbative QCD, the dominant mechanism for producing a single photon with large transverse momentum in a  $pp$  collision is gluon Compton scattering ( $gq \rightarrow \gamma q$ ). The competing partonic subprocess is  $q\bar{q}$  annihilation ( $q\bar{q} \rightarrow \gamma g$ ). Given the predominance of gluons over antiquarks at small Bjorken  $x$ , gluon Compton scattering is ten times more likely to occur. Fig. 3 shows the pQCD predictions for the angular dependence of the cross section and longitudinal spin correlation coefficient for these two processes in the partonic center-of-mass reference frame. The polarized cross section ( $\Delta\hat{\sigma} = \hat{a}_{LL}\hat{\sigma}$ ) is strongly peaked at scattering angles where the

photon is emitted in the direction of the incident quark. This result is independent of the total energy in the partonic CM frame. The best determination of the gluon polarization will be made when the final-state photon is parallel to the initial-state quark; at other angles, there is reduced sensitivity to the gluon polarization.

A second important criterion for optimizing the sensitivity to the gluon polarization is to require large polarizations for the initial-state quark. Measurements<sup>14</sup> of polarized deep-inelastic scattering (DIS) have determined that the quark polarization increases linearly with  $\log x$ , for momentum fractions greater than 0.1. At  $x_q \approx 0.2$ , the quark polarization is  $\sim 0.3$ , and it continues to rise as  $x_q$  increases. Furthermore, we have learned from *unpolarized* DIS, that the small  $x$  region ( $x_q \leq 0.1$ ) is precisely where gluons predominately reside<sup>11</sup>. Hence, the optimum determination of the fraction of the proton's spin carried by gluons will be made by using large- $x$  quarks ( $x_q \geq 0.2$ ) as an *analyzer of the polarization* of small- $x$  gluons.

These two criteria suggest that the greatest sensitivity to  $\Delta G(x)$  results from *asymmetric gluon Compton scattering* ( $x_q > x_g$ ), with the photon detected in the same direction that the partonic CM moves in the collider reference frame. As a consequence, both the photon and the hadronic jet from gluon Compton scattering events should be detected at large pseudorapidity, limited only by the need for large  $p_T$  in the collision, generally assumed to be proportional to the kinematic scale,  $Q$ , relevant for the structure functions. To limit the contributions from higher-twist processes, we will consider below direct photon production with  $p_{T,\gamma} \geq 10$  GeV/c.

## 5.2 Simulating polarized proton collisions

Sophisticated event generators have been developed for high-energy (unpolarized)  $pp$  and  $p\bar{p}$  collisions to aid in the optimization of experiments. To explore

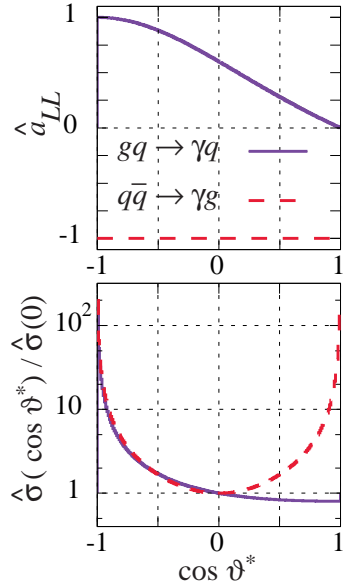


Figure 3: Leading-order perturbative QCD predictions for the partonic spin correlation coefficient and the relative differential cross section for photon production processes. For gluon Compton scattering, the partonic center of mass scattering angle ( $\theta^*$ ) is defined relative to the incident gluon.

questions about the expected performance of the STAR detector we turn to a QCD event generator (PYTHIA 5.7)<sup>15</sup>, known to include many of the salient features of hard scattering processes. Hadronization of the recoiling quarks and gluons following a hard-scattering event is accounted for by the Lund string model, with parameters tuned to agree with fragmentation functions measured in  $e^+e^-$  colliders. The multiple soft-gluon emission, thought to be responsible for the introduction of transverse momentum to the initial-state partons, is accounted for in PYTHIA through the parton-shower model<sup>16</sup>, rather than by explicit evaluation of higher-order QCD processes.

Spin effects are included for each event by evaluating the leading-order pQCD expressions for the process-specific spin-correlation coefficient<sup>17</sup>,  $\hat{a}_{LL}^{proc}$ , using the Mandelstam variables  $(\hat{s}, \hat{t}, \hat{u})$  for the partonic hard scattering, as given by PYTHIA. For the polarization observables, the helicity asymmetry distributions from Gehrmann and Stirling<sup>10</sup> are evaluated at the Bjorken  $x$  values ( $x_{1(2)}$ ) given by PYTHIA, after being evolved<sup>18</sup> to  $Q^2 = p_{T,\gamma}^2/2$ . Gehrmann and Stirling provide three different sets of distributions, referred to here as GS-A, B and C. The sets differ mostly for  $\Delta G(x)$  (Fig. 2). Armed with these variables, the proton spin correlation for a given  $pp$  scattering event is calculated as:

$$A_{LL} = \frac{\Delta f_a(x_1, Q^2)}{f_a(x_1, Q^2)} \frac{\Delta f_b(x_2, Q^2)}{f_b(x_2, Q^2)} \hat{a}_{LL}^{proc}(\hat{s}, \hat{t}, \hat{u}). \quad (5)$$

In this equation,  $\Delta f/f$  is the polarization of the parton (either a gluon or a quark (antiquark) of a given flavor) within one of the interacting protons (either beam  $a$  or  $b$ ), assuming the beams are 100% polarized. The generated event may in principle arise from colliding protons with either equal (+) or opposite (-) helicities, but with different probabilities, proportional to

$$\mu_{\pm} = [1 \pm P_{b_1} P_{b_2} A_{LL}] \sigma_{eff}. \quad (6)$$

In the simulations, the initial helicity state for a given event is chosen randomly in accordance with the above relative probabilities. In Eqn. 6 the beam polarizations,  $P_{b_{1(2)}}$ , are each taken to be equal to 0.7, as expected for the RHIC-spin program. Alternate selection between the two polarization states (representing for two-spin observables either equal or opposite helicity states for the colliding protons) is continued until a non-zero value is drawn, corresponding to the occurrence of a collision.

A key assumption in this method of computing polarization observables, is that initial-state parton showers are spin independent. This assumption has been checked in simulations (SPHINX<sup>19</sup>) that separately consider parton showers independently for each helicity projection of the initial-state partons before the hard scattering. The good agreement<sup>20</sup> between SPHINX and the

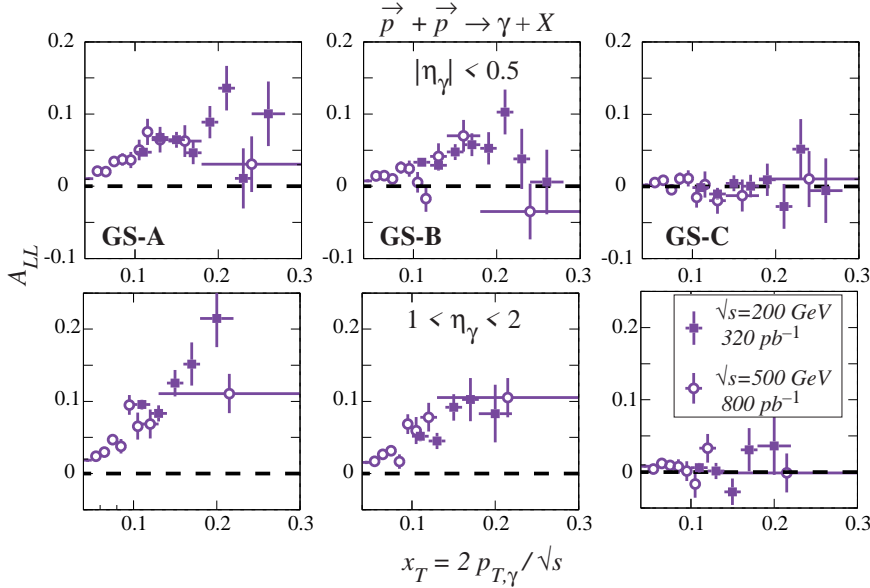


Figure 4: Simulated values for  $A_{LL}$  for inclusive photon production at RHIC energies. The top row shows the spin correlations for midrapidity photons that can be detected at both PHENIX and STAR. The bottom row shows expected values at the forward angles probed by the STAR endcap electromagnetic calorimeter (EEMC). Not evident in this figure, is that for a given  $x_T$ , photons detected in the EEMC correspond to smaller- $x$  gluons than those detected at midrapidity.

method outlined above for the polarization observables suggests minimal spin-dependent effects from the initial-state parton showers. Further support for this conclusion comes from next-to-leading order QCD calculations<sup>21</sup>. Higher-order processes are found to minimally influence the polarization observables computed in leading order. One precaution is that, to date, the necessary resummation, required to account for multiple soft gluon emission, has not yet been carried out for photon production processes.

Given this methodology, polarization observables have been calculated for a variety of processes. The acceptance and finite resolution of the STAR barrel and endcap calorimeters (EMC) for photons is accounted for in these simulations. Isolation criteria<sup>22</sup> are applied to the simulations, anticipating their need in real experiments to reduce backgrounds (Sect. 5.5). Some of the calculations presented below rely on hadronic jet reconstruction. For those calculations, the response of the STAR TPC and the EMC are approximately

accounted for. Standard jet reconstruction algorithms<sup>23</sup> are applied, based on the charged particle tracking from the STAR TPC and the electromagnetic energy detection from the EMC, and assuming that long-lived neutral hadrons ( $n, \bar{n}, K_L^0$ ) are not detected. To avoid edge effects, the reconstructed jet is required to be within a full cone radius (taken to be of size,  $R = 0.7$  radians) from the edge of the STAR detector limits.

The resulting asymmetries for inclusive direct photon production, under the conditions described above, are shown in Fig. 4 as a function of the photon transverse momentum, scaled by  $\sqrt{s}$ . Several observations can be made:

- For the GS-A,B gluon helicity asymmetry distributions, the  $A_{LL}$  values are expected to be ‘large’ ( $> 0.05$ ) for large  $x_T$ , corresponding to values of  $x_g$  where the gluon polarization is large. The small  $A_{LL}$  values for GS-C reflect the small gluon polarization at all  $x_g$ , arising because the peak of  $x\Delta G(x)$  (Fig. 2) occurs at an  $x_g$  value where the unpolarized distribution is already quite large.
- The qualitative features of direct photon production (discussed in Sect. 5.1) are evident by comparing  $A_{LL}$  for midrapidity and forward-angle photons. The latter, in general, results in larger magnitude asymmetries; and hence, a greater sensitivity to  $\Delta G$ .
- It is necessary to detect very hard photons ( $p_{T,\gamma} > 30$  GeV/c) to enable measurements of  $A_{LL}$  at the same  $x_T$  for two values of  $\sqrt{s}$ . Higher energy photon detection is more difficult, but is important to accomplish. Sampling the same  $x_T$  at different  $\sqrt{s}$  is an important check of the theory. Direct photon production cross sections have been shown to deviate from next-to-leading order QCD calculations in an  $x_T$ -dependent manner<sup>24</sup>. One speculation for this is the need for larger  $k_T$  smearing than is present in the theory.

### 5.3 Determining the initial-state partonic kinematics

Direct photon production, where only the photon is detected (inclusive detection), provides only crude determination of the initial-state partonic kinematics. It is generally assumed for photons detected at mid-rapidity ( $\eta \approx 0$ ), that the kinematic quantity  $x_T = 2p_{T,\gamma}/\sqrt{s}$  is approximately equal to the Bjorken  $x$  values of the initial-state colliding partons. This assumption is only approximately valid for the *average values* of  $x_g$  and  $x_q$ . In fact, due to the lack of any constraint on the direction of the recoiling jet,  $x_g$  and  $x_q$  are distributed along an approximately hyperbolic locus at fixed  $x_T$  and  $\eta_\gamma$ . This locus is slightly broadened by  $k_T$  smearing effects.

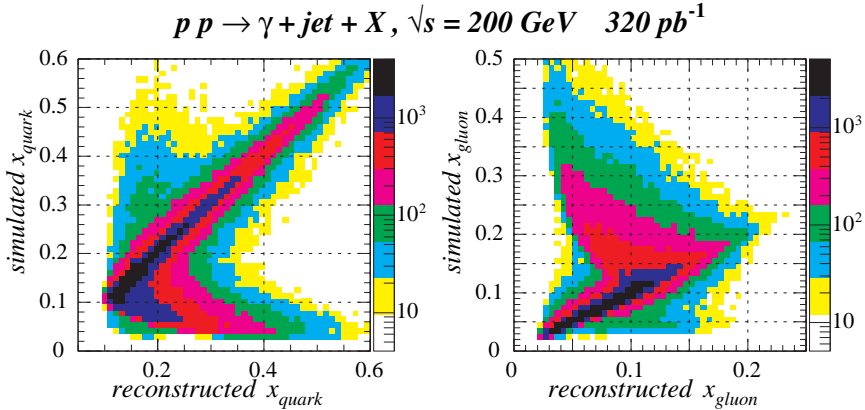


Figure 5: Correlation between reconstructed and simulated values for the quark and gluon momentum fractions for the  $p + p \rightarrow \gamma + \text{jet} + X$  reaction. The simulations include effects of  $k_T$  smearing. The reconstruction assumes collinear collisions. Only events with an isolated photon in the STAR acceptance ( $-1 \leq \eta \leq 2$ ) having  $10 \leq p_T \leq 20 \text{ GeV}/c$  are accepted. The coincident jet must be within the fiducial volume of STAR ( $-0.3 \leq \eta_{\text{jet}} \leq 1.3$ ). A further restriction that the reconstructed  $x_{\text{quark}} \geq 0.2$  is also imposed.

These kinematic ambiguities can be vastly reduced by detecting the away-side jet in coincidence with the photon. With the reasonable assumption of collinearity of the colliding partons in the initial state, it is easy to show that the initial-state momentum fractions can be determined for each event by measuring the energy ( $p_{T,\gamma}$ ) and direction of the photon ( $\eta_\gamma$ ), and only the direction of the away-side hadronic jet ( $\eta_{\text{jet}}$ ). With this information, conservation of energy and momentum at the partonic level imply

$$x_1 = \frac{x_T}{2}(e^{-\eta_\gamma} + e^{-\eta_{\text{jet}}}) \quad \text{and} \quad x_2 = \frac{x_T}{2}(e^{+\eta_\gamma} + e^{+\eta_{\text{jet}}}). \quad (7)$$

Given the measured quark and gluon helicity-independent probability distributions, the reasonable assumption is made that the initial-state quark had momentum fraction  $x_q^{\text{recon}} = \max[x_1, x_2]$  and the gluon,  $x_g^{\text{recon}} = \min[x_1, x_2]$ . Similarly, it is straightforward to express the partonic CM scattering angle in terms of  $\eta_\gamma$  and  $\eta_{\text{jet}}$ . A key assumption, that is examined more carefully below, is that the initial-state partons are collinear. A valid question is, to what extent do transverse momentum components in the initial state ( $k_T$ ) interfere with the event-by-event determination of the kinematics?

To address this question, the reconstruction algorithm was applied to PYTHIA simulations of direct photon processes. The initial-state partons had

transverse momentum components, as generated by the parton shower model. Events having at least one jet and a coincident photon within the STAR fiducial volume were reconstructed. The UA2 isolation condition<sup>22</sup> was applied to the photon. A condition that the reconstructed  $x_q$  was greater than 0.2 was also imposed. As is evident in Fig. 5, most of the events have the initial-state momentum fractions properly reconstructed. The majority of the kinematic reconstruction errors occur when  $x_q < x_g$ .

#### 5.4 Direct reconstruction of $\Delta G(x)$

Armed with the knowledge that the initial-state partonic kinematics can be accurately reconstructed, it is possible to consider *directly reconstructing  $\Delta G(x)$  from the measured longitudinal spin correlation*. It is possible that such a direct reconstruction will provide the best framework for deducing  $\Delta G$  from photon production measurements. As is already evident from Eqn. 5, if only quark-gluon Compton scattering contributes to the photon yield, then

$$A_{LL} = \frac{\Delta G(x_g, Q^2)}{G(x_g, Q^2)} A_1^p(x_g, Q^2) \hat{a}_{LL}^{\text{Compton}}(\theta^*). \quad (8)$$

This equation results from Eqn. 5, when averaging over an event ensemble, since the  $u$  and  $d$  quark contributions to gluon Compton scattering are weighted by their squared electric charge and the probability to find them inside the proton. This is identical to the weighting that enters in polarized deep-inelastic scattering (PDIS). The quantity,  $A_1^p$ , in Eqn. 8 is then precisely the asymmetry measured in PDIS<sup>14</sup>.

Since the kinematics can be determined for individual events, it is possible to invert Eqn. 8 to express the reconstructed gluon helicity asymmetry distribution in terms of *known* quantities: the unpolarized gluon PDF, the quark polarization and the pQCD expression for the gluon Compton scattering partonic spin correlation; and the measured spin-dependent scattering yields ( $N_{++}^{(+-)}$ ):

$$\Delta G_{\text{recon}}(x_g) = \frac{[N_{++}(x_g) - N_{+-}(x_g)]}{P_{b_1} P_{b_2} \sum_{i=1}^{N_{++} + N_{+-}} [A_1^{\text{DIS}}(x_{q_i}, Q_i^2) \hat{a}_{LL}^{\text{Comp.}}(\theta_i^*) / G(x_{q_i}, Q_i^2)]}. \quad (9)$$

This inversion, as applied to simulations of  $A_{LL}$  for direct photon processes is shown in Fig. 6. The key assumptions implicit to this direct reconstruction, and their influence on  $\Delta G_{\text{recon}}(x)$ , are:

- *Only the gluon Compton process contributes to the  $\gamma$ +jet yield; the other processes that contribute to the simulated yields are assumed to be absent*

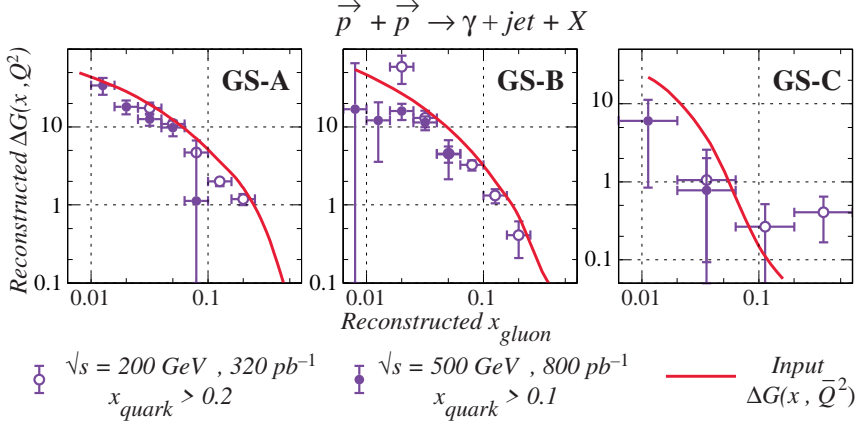


Figure 6: Results for the direct reconstruction of  $\Delta G(x, Q^2)$ , as applied to the simulated values of  $A_{LL}$  for direct photon processes. Three different inputs for  $\Delta G(x)$  are shown.

in the reconstruction. The small contribution from  $q\bar{q} \rightarrow \gamma g$  is negative, and is proportional to the product of the quark and antiquark polarizations at the asymmetric Bjorken  $x$  values probed in the experiment. This contribution results in  $\Delta G_{recon}(x)$  underestimating the input value of  $\Delta G(x)$ .

- The initial-state partonic kinematics are assumed to be perfectly reconstructed. For some events, especially the small number with  $x_g > x_q$ , there are reconstruction errors. Typically,  $A_{LL}$  for the  $x_g$  value reconstructed for these events is smaller than for those events that don't have kinematic reconstruction errors. The end result is that  $\Delta G_{recon}(x)$  underestimates the input value of  $\Delta G(x)$ .
- The partonic collisions are assumed to be collinear, so  $k_T$  smearing effects are assumed to be absent. These effects introduce non-zero transverse momentum in the initial state, contrary to the assumption of collinear collisions. The end result is to make correlated errors in the reconstruction of  $x_q$  and  $x_g$ .

Corrections to  $\Delta G_{recon}(x)$  for these three effects can be made based on simulations. The first correction requires no knowledge of  $\Delta G(x)$ , whereas the latter two would need to be made in an iterative fashion, since knowledge of  $\Delta G(x)$  is required.

In addition to these three effects, present in the results shown in Fig. 6, other effects can influence  $\Delta G_{recon}(x)$  that will be determined from  $\vec{p} + \vec{p} \rightarrow \gamma + jet + X$  data. In particular, the  $\gamma\gamma$  decay of a high-energy  $\pi^0(\eta)$  meson can mimic the detector response of a single high-energy photon. Simulations<sup>8</sup> have shown that this background results in a smaller magnitude  $A_{LL}$  compared to direct photon production, and if not properly corrected, would result in an underestimate of the true  $\Delta G(x)$  via the direct reconstruction method. Another problem facing the RHIC-spin experiments, is the possibility that some fraction of the photons produced in  $\vec{p} + \vec{p}$  collisions arise from the ‘fragmentation’ of recoiling final state partons. In particular, high- $p_T$  photons can be produced in the hard bremsstrahlung of a charged parton, produced by  $qg$  or  $gg$  scattering processes that have significantly larger cross section than the direct photon processes. Simulations<sup>25</sup> have shown that these other processes will dilute the direct photon  $A_{LL}$  by a small amount. Again, they tend to underestimate the true  $\Delta G(x)$  via the direct reconstruction method.

### 5.5 Backgrounds and their suppression

To employ direct photon production as a means of determining the polarization of the proton’s glue, a detector must be capable of selecting the very small fraction of events that have a single high energy photon. The most pernicious physics background arises from di-jet events (by far, the largest fraction of the total reaction cross section), where one of the jets has an energetic neutral meson ( $\pi^0$  or  $\eta^0$ , collectively referred to as  $M^0$ ) that can decay into a pair of photons. Kinematically, the most probable opening angle between the photons produced by  $M^0$  decay is  $\phi_{\gamma\gamma}^{\min} = 2\sin^{-1}(m_{M^0}c^2/E_{M^0})$ . For a 30 GeV  $\pi^0$  this angle is 9 mr. Such a small opening angle makes it very difficult for any detector to distinguish between di-photons from  $M^0$  decay and a single direct photon.

The relative probability for producing a neutral meson versus a direct photon is shown in Fig. 7a. Due to the larger number of processes that can produce jets versus single photons, and the fact that the strong interaction coupling constant ( $\alpha_S$ ) is involved rather than the electromagnetic coupling constant ( $\alpha$ ),  $M^0$  production is nearly an order of magnitude larger than  $\gamma$  production. This result from PYTHIA has been shown<sup>25</sup> to be roughly in accord with existing measurements<sup>26</sup>.

The influence of the  $M^0$  background on the direct photon measurements at RHIC is different for the PHENIX and STAR detectors. The former has a smaller solid angle, but substantially finer granularity, EMC than the latter. This feature allows PHENIX to better reconstruct  $M^0$  from their daughter

photons. The uniform distribution of the decay photon energies from  $M^0$  decay ultimately sets a limit to the range of decay phase space where this background suppression technique is effective. The STAR detector will distinguish background from signal using two primary techniques, described below.

The first of the background suppression methods for STAR relies on a ‘shower maximum detector’ (SMD)<sup>8</sup>. This is a fine granularity detector placed within the depth of the calorimeter to measure the transverse profile of the electromagnetic (EM) showers produced by the incident particles. In general, an incident  $M^0$  results in two separated clumps of energy deposition in the SMD, corresponding to the spatial separation of the EM showers produced by the closely spaced daughter photons. An incident direct photon typically produces only a single clump of energy deposition in the SMD<sup>8</sup>. This distinction is muddied by the complexity of EM showers, resulting in false clumpiness in the SMD response for some fraction of the direct-photon-induced events. Despite this, the analysis of the SMD information will provide significant suppression of the  $M^0$  background.

The second component of the background suppression arsenal of STAR is related to the nearly  $4\pi$  coverage the detector provides. In general, high energy neutral mesons are leading particles of jets, and hence, are accompanied by additional hadrons. An effective discrimination between  $M^0$  and direct photon events is provided by examining the event topology. The former class of events generally have additional hadrons within a relatively narrow cone around the  $M^0$  whereas direct photon events have little accompanying energy within the isolation cone. The  $M^0$  events can be suppressed by using ‘isolation cuts’ similar to those used in other collider detectors reporting direct photon cross sections.

The influence of these background reduction cuts on the background:signal

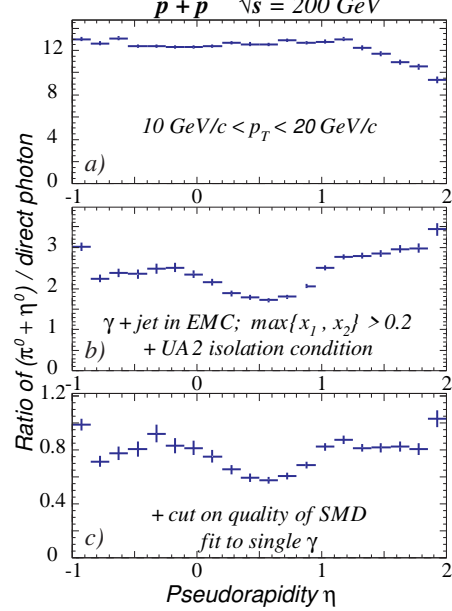


Figure 7: Ratio of cross sections for  $\pi^0(\eta)$  and direct photon production under increasingly stringent conditions: a) including only a  $p_T$  cut; b) cuts on kinematic quantities and an isolation cut; c) cut on information from SMD.

ratio is illustrated in Figs. 7b and 7c. The end result is that the signal is expected to be approximately  $2\times$  larger than the background. The remaining background contributions can be eliminated by taking the difference between distributions enriched in direct photons and those enriched in  $M^0$ . This subtraction process will increase the statistical errors beyond those shown in Fig. 6 by a factor varying between 1.5 and  $2^8$ . The systematic error associated with these corrections can be estimated from *in situ* calibrations of the performance of the SMD, made possible by producing an energetic  $\pi^0$  sample from reconstructed  $\rho^\pm$  events. Other backgrounds will also be present in both the STAR and PHENIX experiments, but their effects on the determination of  $\Delta G$  should be less important. Efforts are underway to understand the limitations on extracting  $\Delta G$  from direct photon measurements.

### 5.6 Extrapolation Errors

Unlike the goals of most experiments sensitive to gluon polarization that are either underway<sup>13</sup> or are on the horizon<sup>12</sup>, the RHIC-spin program aims to determine the *integral contribution* gluons make to the proton's spin, as defined in Eqn. 1. To carry out this integral, the gluon helicity asymmetry distribution must be determined over a sufficiently broad range of  $x_g$  to minimize the influence of extrapolation errors in carrying out the integral over all  $x$ . To illustrate how these errors influence the determination of  $\Delta G$ , a standard parameterization of the  $x_g$  dependence,

$$x\Delta G(x) = \eta Ax^a(1-x)^b[1+\rho x^{1/2}+\gamma x],$$

with  $A^{-1} = \left(1 + \frac{\gamma a}{a+b+1}\right) \frac{\Gamma(a)\Gamma(b+1)}{\Gamma(a+b+1)} + \rho \frac{\Gamma(a+\frac{1}{2})\Gamma(b+1)}{\Gamma(a+b+1)}$ , (10)

so that  $\eta = \int_0^1 \Delta G(x)dx$ ,

is fit to simulated data. Similar to the method used to analyze existing data on scaling violations in polarized deep inelastic scattering<sup>10</sup>,  $b$  and  $\gamma$  are held fixed at values obtained by evolving<sup>18</sup> the  $\Delta G(x)$  input to the simulation to the  $Q^2$  values relevant at RHIC. The fixed parameters used in the fits are consistent with positivity constraints ( $|\Delta G(x)| < G(x)$ ). The parameters  $\eta, a, \rho$  are then adjusted to provide the best fit to  $\Delta G_{recon}(x)$ , described in Sect. 5.4. The results for the simulations of the  $\sqrt{s}=200$  and 500 GeV samples are combined, after making additive corrections for  $q\bar{q}$  annihilation contributions to the simulated asymmetries. No corrections have been made for kinematic reconstruction errors or  $k_T$  smearing. As well, the values of  $\Delta G_{recon}(x)$  have

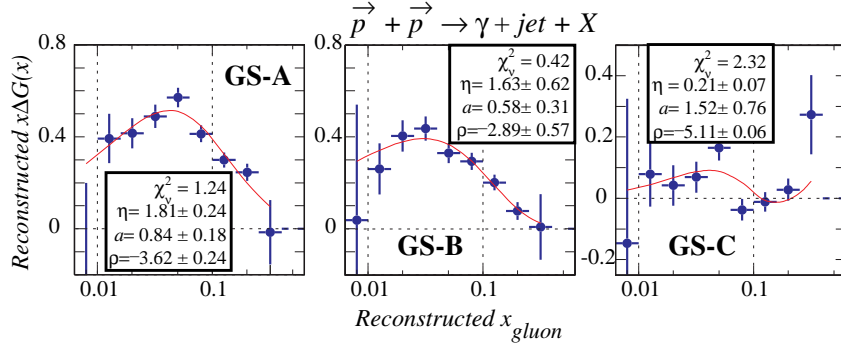


Figure 8: Fits to the reconstructed  $\Delta G(x)$ , after correcting for  $q\bar{q}$  annihilation. A standard parameterization (Eqn. 10) is used to fit the data, with the  $b$  and  $\gamma$  parameters fixed. Full data sets for  $\sqrt{s}=200(500)$  GeV are assumed, corresponding to integrated luminosity of  $320(800)$  pb $^{-1}$ .

not been evolved to a common  $Q^2$ . These corrections are important, but have not been made because they require knowledge of  $\Delta G(x)$ . The fits are shown in Fig. 8. It is found that:

- *an accurate determination of  $\Delta G$  will require both  $\sqrt{s}=200$  and 500 GeV data samples to get to sufficiently small  $x_g$ .* Due to strong correlations between  $\eta$  and  $a$ ,  $\delta\eta$  grows rapidly as the low- $x$  points are successively eliminated. The error in the integral  $\Delta G$  ( $\delta\eta$ ), with both samples included in the fit, is 0.24 when Gehrmann-Stirling<sup>10</sup> set A is input to the simulations. The value for  $\delta\eta$  for set B is 0.62, and the relative error in  $\eta$  is comparable for set C. For set A, other systematic errors are expected<sup>8</sup> to increase the error in the integral  $\Delta G$  to 0.5, still sufficient to accurately establish  $\Delta\Sigma$  from polarized deep inelastic scattering.
- *the large- $x$  behavior of  $\Delta G(x)$  must be constrained to determine  $\Delta G$  at RHIC.* Different values for the fixed parameters ( $b, \gamma$ ) result in different values for  $\eta$ .
- *fitting  $\Delta G_{recon}(x)$ , including only the corrections for  $q\bar{q}$  annihilation, yields a value for the fitted  $\eta$  that is too small compared to the input  $\Delta G$ .* Evolving all of the  $\Delta G_{recon}(x)$  points to a common  $Q^2$  and correcting for the kinematic reconstruction errors results in a fitted  $\eta$  that is closer to the input  $\Delta G$ , but is still too small. Both of these corrections require knowledge of  $\Delta G(x)$ , and hence will require an iterative procedure for their application. The largest remaining error comes from  $k_T$  smearing.

Repeating the analysis with simulations that don't include initial-state parton showers results in a fitted  $\eta$  in agreement with the input  $\Delta G$ .

The end result is, that after accounting for the most significant sources of systematic error<sup>8</sup>, we expect that the fraction of the proton's spin carried by gluons can be determined to an accuracy of approximately 0.5, primarily based on the STAR measurements of  $\vec{p} + \vec{p} \rightarrow \gamma + \text{jet} + X$ . Data samples at both  $\sqrt{s}=200$  and 500 GeV are crucial so that the accuracy is not limited by extrapolation errors. The analysis of  $\Delta G_{\text{recon}}(x)$  presented here is intended to illustrate the sensitivity of the STAR measurements to the integral  $\Delta G$ . Clearly, the best determination of  $\Delta G$  will result from a global analysis of all relevant data.

## 6 Summary

The RHIC-spin program promises to provide exciting data to test perturbative QCD, and to provide new insights into the non-perturbative structure of the proton. It is likely that one of the most interesting results will be the determination of the fraction of the proton's spin carried by gluons. I expect that inclusion of  $\Delta G_{\text{recon}}(x)$ , based on the measurement of  $A_{LL}$  for the  $\vec{p} + \vec{p} \rightarrow \gamma + \text{jet} + X$  reaction at  $\sqrt{s}=200$  and 500 GeV, in a global analysis will provide the best determination of the gluon contribution to the proton's spin.

## Acknowledgments

I gratefully acknowledge the extensive discussions I've had with my IUCF colleagues (W.W. Jacobs, J. Sowinski, E.J. Stephenson, S.E. Vigdor and S.W. Wissink) while carrying out this work. I also thank my colleagues for their careful reading of, and comments on, this manuscript.

## References

1. M.Bai *et al*, *Phys. Rev. Lett.* **80**, 4673 (1998).
2. C. Bourrely and J. Soffer, *Phys. Lett. B* **314**, 132 (1993).
3. P. Taxil and J.M. Virey, *Phys. Lett. B* **364**, 181 (1995).
4. D.L. Adams *et al*, *Phys. Lett. B* **264**, 462 (1991).
5. R.L. Jaffe, in Proc. 2nd Topical Workshop on Deep Inelastic Scattering off Polarized Targets, DESY, 1997 (preprint hep-ph/9710465).
6. Ya. S. Derbenev and A.M. Kondratenko, *Part. Accel.* **8**, 115 (1978).
7. A. D. Krisch *et al*, *Phys. Rev. Lett.* **63**, 1137 (1989).
8. L.C. Bland, W.W. Jacobs, J. Sowinski, S.E. Vigdor and S.W. Wissink, STAR Note 401 (1999).

9. D. Adams *et al*, *Phys. Rev. D* **56**, 5330 (1997).
10. T. Gehrmann and W.J. Stirling, *Phys. Rev. D* **53**, 6100 (1996).
11. A. de Roeck, in these proceedings.
12. A. Bravar, D. von Harrach and A. Kotzinian, *Phys. Lett. B* **421**, 349 (1998).
13. A. Bruell, in these proceedings.
14. M. Petratos, in these proceedings.
15. T. Sjöstrand, *Comp. Phys. Commun.* **82**, 74 (1994).
16. T. Sjöstrand, *Phys. Lett. B* **157**, 321 (1985).
17. C. Bourrely, J. Soffer, F.M. Renard and P. Taxil, *Phys. Rep.* **177**, 319 (1989).
18. M. Hirai, S. Kumano and M. Miyama, *Comp. Phys. Commun.* **108**, 38 (1998).
19. S. Güllenstern *et al*, unpublished (1997).
20. O. Martin, in Proc. of 2nd workshop on Event Generators for RHIC Spin Physics, RIKEN/BNL, 1999.
21. L.E. Gordon and W. Vogelsang, *Phys. Rev. D* **170**, 1994 (.)
22. J. Alitti *et al*, *Phys. Lett. B* **299**, 174 (1993).
23. W.B. Christie and K. Shesternov, STAR Note 196 (1995).
24. J. Huston *et al*, *Phys. Rev. D* **51**, 6139 (1995).
25. L.C. Bland, in Proc. of 2nd workshop on Event Generators for RHIC Spin Physics, RIKEN/BNL, 1999.
26. M.E. Beddo, H. Spinka and D.G. Underwood, STAR Note 77 (1992).